physica status solidi b
www.pss-b.com
basic solid state physics

Broadband viscoelastic spectroscopy measurement of mechanical loss and modulus of polycrystalline $BaTiO_3$ vs. temperature and frequency

Liang Dong[1], Donald S. Stone[1], and Roderic S. Lakes[2]

[1] Department of Materials Science, University of Wisconsin-Madison, Madison, WI 53706-1687, USA
[2] Department of Engineering Physics, Engineering Mechanics Program, Biomedical Engineering Department, Material Science Program and Rheology Research Center, University of Wisconsin-Madison, Madison, WI 53706-1687, USA

Received 17 June 2008, revised 8 August 2008, accepted 20 August 2008
Published online 15 October 2008

PACS 62.20.de, 77.80.–e, 77.84.Cy

Characterization of pure polycrystalline $BaTiO_3$ was carried out by means of Broadband Viscoelastic Spectroscopy (BVS) and Differential Scanning Calorimetry (DSC) above ambient temperature. A peak in mechanical loss has been observed near the Curie point 130 °C. The magnitude of the peak increases with thermal rate and decreases with frequency. Expressions for the peak magnitude have been derived based upon available models describing the first order phase transition. Mechanical anomalies were observed outside the vicinity of the phase transition. Transition temperature measured by BVS differed from that via DSC; the effect of stress on the ferroelastic transformation is a possible cause. Isothermal frequency scans revealed a hump in mechanical loss in the vicinity of the transition temperature below 1 Hz and a modulus decrease with decreasing frequency. Quasi-isothermal studies revealed a significant softening in bulk modulus and a transient negative Poisson's ratio during the tetragonal-to-cubic phase transition.

phys. stat. sol. (b) **245**, No. 11, 2422–2432 (2008) / **DOI** 10.1002/pssb.200880270

phys. stat. sol. (b) **245**, No. 11, 2422–2432 (2008) / **DOI** 10.1002/pssb.200880270

physica status solidi b
www.pss-b.com
basic solid state physics

Broadband viscoelastic spectroscopy measurement of mechanical loss and modulus of polycrystalline $BaTiO_3$ vs. temperature and frequency

Liang Dong[1], Donald S. Stone[1], and Roderic S. Lakes[*,2]

[1] Department of Materials Science, University of Wisconsin-Madison, Madison, WI 53706-1687, USA
[2] Department of Engineering Physics, Engineering Mechanics Program, Biomedical Engineering Department, Material Science Program and Rheology Research Center, University of Wisconsin-Madison, Madison, WI 53706-1687, USA

Received 17 June 2008, revised 8 August 2008, accepted 20 August 2008
Published online 15 October 2008

PACS 62.20.de, 77.80.–e, 77.84.Cy

[*] Corresponding author: e-mail lakes@engr.wisc.edu

Characterization of pure polycrystalline $BaTiO_3$ was carried out by means of Broadband Viscoelastic Spectroscopy (BVS) and Differential Scanning Calorimetry (DSC) above ambient temperature. A peak in mechanical loss has been observed near the Curie point 130 °C. The magnitude of the peak increases with thermal rate and decreases with frequency. Expressions for the peak magnitude have been derived based upon available models describing the first order phase transition. Mechanical anomalies were observed outside the vicinity of the phase transition. Transition temperature measured by BVS differed from that via DSC; the effect of stress on the ferroelastic transformation is a possible cause. Isothermal frequency scans revealed a hump in mechanical loss in the vicinity of the transition temperature below 1 Hz and a modulus decrease with decreasing frequency. Quasi-isothermal studies revealed a significant softening in bulk modulus and a transient negative Poisson's ratio during the tetragonal-to-cubic phase transition.

1 Introduction The classical bounds [1] for composite properties such as modulus, mechanical loss or thermal expansion, which are derived under the assumption that both matrix and inclusion possess positive stiffness, state that these properties cannot surpass those of constituents. However, such bounds can be exceeded given the existence of negative-stiffness inclusions [2]. Negative stiffness is presented as the occurrence of a reaction force in the same direction as imposed deformation, and is achieved by stored energy at quasi-equilibrium [2]. Jaglinski et al. [3] studied a composite material, of polycrystalline $BaTiO_3$ particle inclusions embedded in tin matrix, which attained a stiffness (Young's modulus) almost ten times greater than that of diamond via inclusions capable of the "tetragonal ↔ cubic" phase transition. The extreme stiffness was attributed to the negative bulk modulus of this ferroelastic inclusion during its phase transition. With the aim of directly observing the softening of the bulk modulus hypothesized in the design of the above composite, we have studied the mechanical properties (modulus and the corresponding mechanical loss) of pure polycrystalline $BaTiO_3$ by means of Broadband Viscoelastic Spectroscopy (BVS).

To examine the trend of the viscoelastic properties in $BaTiO_3$ ceramic near the "tetragonal ↔ cubic" phase transition, two sets of experiments were undertaken: (1) Thermal scans were performed in which the temperature of the specimen was either raised or lowered through the Curie point while the viscoelastic properties (mechanical loss and modulus) were measured at fixed excitation frequency. Theories (see Table 1 in Ref. [4]) predict that mechanical loss will depend on both the rate of temperature change and the excitation frequency at which the viscoelastic properties are measured. Our observations are in accordance with those theories and the previous experimental reports on $BaTiO_3$ ceramic [5, 6] as it undergoes the "tetragonal ↔ cubic" phase transition. (2) Isothermal broadband viscoelastic spectroscopy tests were performed measuring the viscoelastic properties of the specimen at temperatures near the Curie point and as a function of the

excitation frequency spanning almost six decades. These experiments allowed us to examine in detail the properties of polycrystalline $BaTiO_3$ over a range of conditions hitherto unexplored. They also allowed us to minimize the thermal gradient in the specimen inherent to temperature scans. To help in understanding the viscoelastic measurements, differential scanning calorimetry was carried out to identify the exact transition temperature.

2 Experimental method A $BaTiO_3$ specimen with a bar shape was sectioned from a large polycrystalline $BaTiO_3$ rod by means of a BUEHLER ISOMET low speed diamond saw. The rod was sintered from Ticon-HPB powder (Ferro Electronic Materials, Niagara Falls, NY) at 1350 °C for 1 hour. The specimen was then polished into regular shape. Its final dimension was 28.94 mm length with rectangular cross section of 2.45 × 2.79 mm, and its density was found to be 5.43×10^3 kg/m^3. The Young's modulus, shear modulus, and mechanical loss of this specimen were measured by means of BVS from ambient temperature to 160 °C at sub-resonant frequencies (10 Hz, 20 Hz, 50 Hz), and from 0.001 Hz to approaching natural frequencies isothermally. Broadband Viscoelastic Spectroscopy (BVS) [7] is capable of studying viscoelastic properties of thermorheologically complex materials, in both torsion and bending, over eleven decades of time and frequency in an isothermal environment or by scanning a single frequency over time while the temperature is varied. Oscillatory torsional or bending torques were applied by driving a sinusoidally varying voltage across the appropriate set of Helmholtz coils using either a function generator (Stanford Research model DS345), or a lock-in amplifier (Stanford Research Systems SR850). This Helmholtz coil imposed a magnetic field on the permanent magnet and transmitted an axial torque on the specimen. The angular displacement of the specimen was measured using laser light reflected from a mirror mounted on the magnet to a split-diode light detector. The detector signal was amplified with a wide-band differential amplifier. Torque was inferred from the Helmholtz coil current as follows. Calibration experiments were done using the well-characterized type 6061 Al alloy, which has well known moduli. Viscoelastic properties (mechanical losses and moduli) of the specimen below resonance were inferred from the amplitude and phase measurements from the lock-in amplifier and were confirmed via phase measurements upon elliptic Lissajous figures. of torque signal vs. angular displacement signal. Temperature was controlled via electrical input to resistance heaters which warmed a suitable amount of flowing air directed into the apparatus. The air flow subsequently served to heat up the specimen. Three identical thermocouples (OMEGA L-0044 K type) were used to measure the temperature, the tips of which were attached to the surface of the specimen by a thin layer of super glue (LOCTITE 409 instant glue), and located separately at the top, middle, and base parts of the specimen. To minimize the effect of the thermal gradient, two methods were applied: (1) wrapping a heating tape (Watlow Columbia Inc. Columbia, MO) onto the lateral surface of a cylindrical brass tube accommodating BVS coils; (2) wrapping a heating cord (Fibrox Inc. Dubuque, IA) onto the top of the BVS support rod. The strain amplitude for each measurement was about 3×10^{-5}.

DSC (Power-Compensated Differential Scanning Calorimeter 7 Perkin Elmer) thermal analysis tests (with rates of 2 °C/min, 5 °C/min, 10 °C/min, 20 °C/min, and 40 °C/min) were conducted on two samples coming from a residual piece which was originally located adjacent to the BVS specimen in the large rod. Samples were named in sequence as I, II. To eliminate the thickness effect on the transition temperature, these two samples were finally ground into similar dimensions using sanding papers. Dimensions for I and II are 2.59 × 1.68 × 0.7 mm, 2.64 × 1.67 × 0.66 mm ($a \times b \times t$), respectively. a, b, t represent length, width, and thickness.

Reflection optical microscopy observation (Nikon Eclipse 80i light microscope with Nikon DXM1200F digital camera, Japan) was performed on a piece from the large rod mechanically ground with SiC abrasive papers from 200 grit down to 1200 grit and finally polished with 1 μm commercial diamond paste on a nap cloth. 100 ml of 5% HCl with several droplets of 48% HF served as the etchant following the method of Kulcsar [8].

3 Results

3.1 Optical micrograph Optical microscopy observation disclosed a grain size distribution from 10 μm to 30 μm. Domain width is less than 2 μm, but is not uniform (Fig. 1). Pores exist since the density of this rod is lower than the theoretical value 6.02×10^3 kg/m^3.

3.2 BVS temperature scans On consideration of the article length, only the 10 Hz BVS temperature scan test results are given, as shown in Figs. 2 and 3, which represent the mechanical losses and the corresponding moduli of this polycrystalline $BaTiO_3$ specimen over a range of temperature from the ambient to above the Curie point.

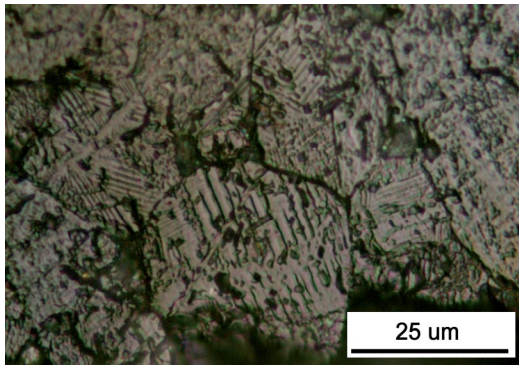

Figure 1 (online colour at: www.pss-b.com) Microstructure of polycrystalline $BaTiO_3$ by means of reflection optical microscopy in polarized light. Etched 2.5 min.

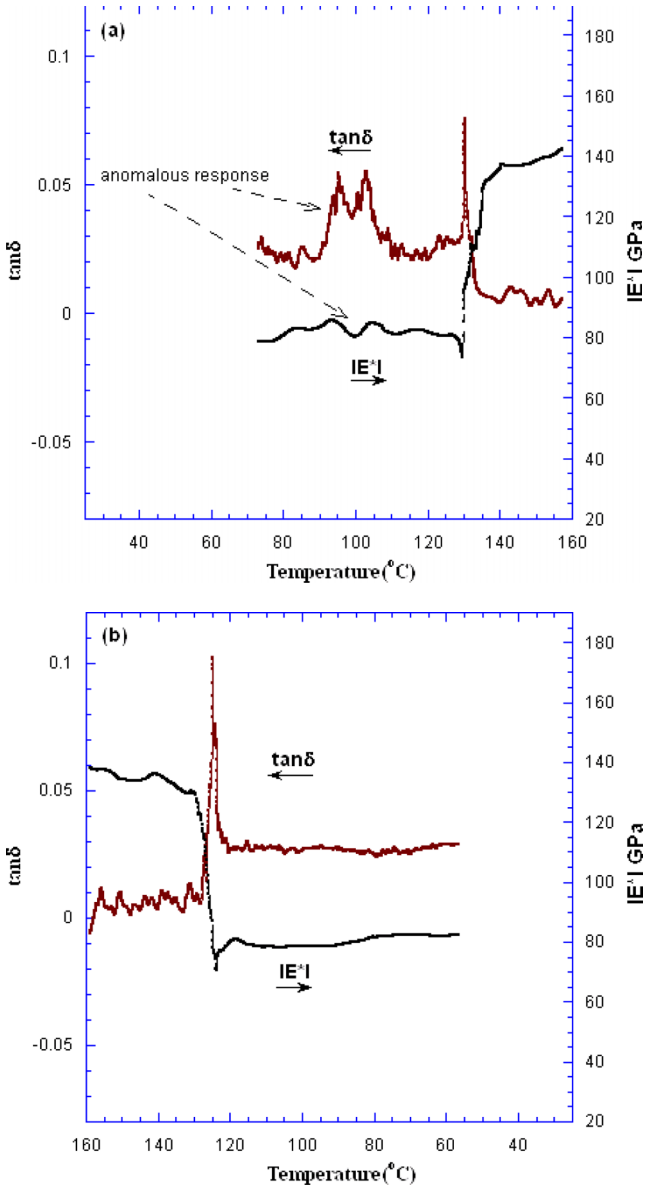

Figure 2 (online colour at: www.pss-b.com) Mechanical loss and Young's modulus vs. temperature curves at 10 Hz frequency during heating (a) with $T' = 0.09$ °C/s and cooling (b) with $T' = -0.08$ °C/s in polycrystalline $BaTiO_3$.

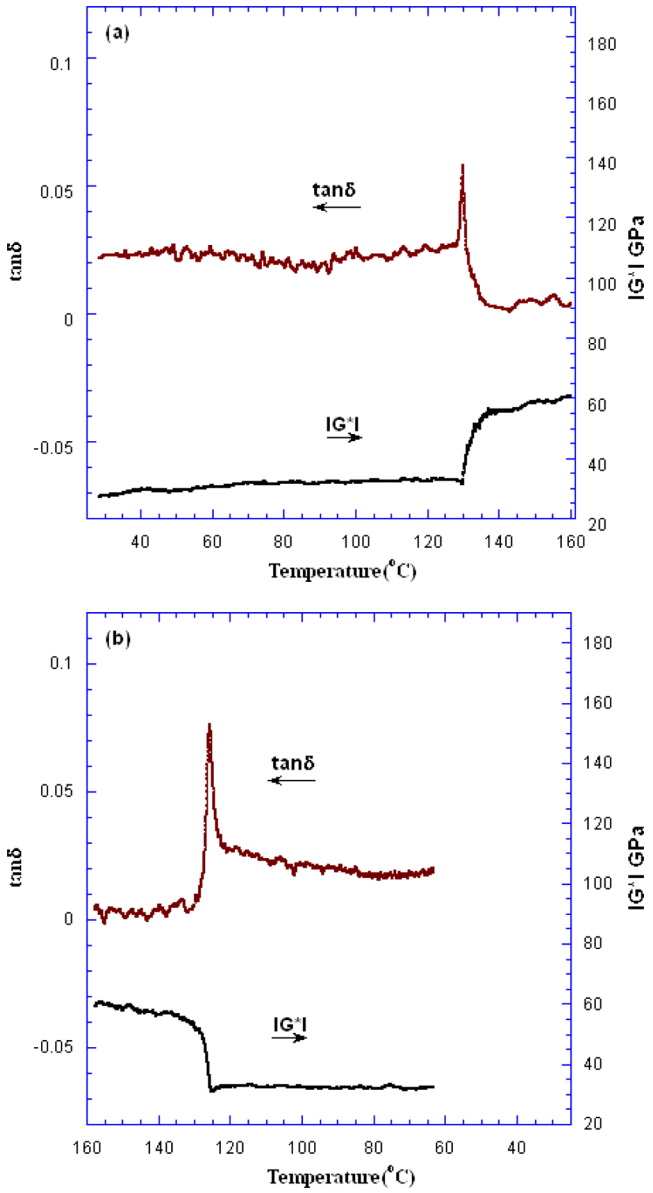

Figure 3 (online colour at: www.pss-b.com) Mechanical loss and shear modulus vs. temperature curves at 10 Hz frequency during heating (a) with $T' = 0.08$ °C/s and cooling (b) with $T' = -0.08$ °C/s in polycrystalline $BaTiO_3$.

The rate of temperature change and the thermal gradient along the axial direction of the specimen were about 0.09 °C/s and 2 °C, respectively, for Fig. 2(a), −0.08 °C/s and 2.6 °C, respectively, for Fig. 2(b), 0.08 °C/s and 2.5 °C, respectively, for Fig. 3(a), and −0.08 °C/s and 1 °C, respectively, for Fig. 3(b).

A peak in mechanical loss, i.e., tan δ (δ is the phase angle between the stress and strain sinusoids), was observed during each of the BVS temperature scan tests near the Curie point 130 °C corresponding to the "tetragonal ↔ cubic" phase transition, which is categorized as a first order phase transition (FOPT) [9]. The height of this peak increases with increasing thermal rate and decreasing frequency. The peak tends to be higher in cooling than in heating given comparable thermal configurations. The peak is also higher in bending than in torsion. The peak width has the tendency to broaden as thermal rate is increased but becomes slightly narrower with increasing frequency. Peak width is also slightly broader in cooling than in heating given comparable thermal and mechanical configurations. The observed dependence of the magnitude of tan δ at T_p (peak temperature) with thermal rate and frequency present the commonly known characteristics of the mechanical loss during a FOPT [10].

The expressions for $(\tan\delta)_{T_p}$, from 10 Hz to 50 Hz in both bending and torsion vibrations, have been derived as follows:

– in bending:

$$(\tan\delta)_{T_p} = 0.964(T')^{0.28}/(2\pi f)^{0.54} + 0.000133(2\pi f)^{0.74} + 0.55 \times 0.027\, e^{0.012f} + 0.45 \times 0.0082\, e^{0.027f}, \quad (1)$$

($10\ \text{Hz} \le f \le 50\ \text{Hz}$, given natural frequency of 590 Hz);

– in torsion:

$$(\tan\delta)_{T_p} = 0.69(T')^{0.24}/(2\pi f)^{0.54} + 0.00011(2\pi f)^{0.7} + 0.55 \times 0.026\, e^{0.005f} + 0.45 \times 0.004\, e^{0.015f}, \quad (2)$$

($10\ \text{Hz} \le f \le 50\ \text{Hz}$, given natural frequency of 5959 Hz), in which T' and f represent thermal rate and frequency, respectively. Owing to curve fitting methods, the last two terms in expressions (1) and (2) are claimed to be valid only within the frequency range specified. The specific procedure and relevant discussion for the derivation of these two expressions are provided in Section 4.1.1.

Anomalous behaviors were observed in some of the tests within certain temperature regions other than in the vicinity of the transformation. Such behaviors were represented as the anomalous responses in mechanical losses and the corresponding moduli within those temperature regions (e.g. temperature region between 90 °C and 110 °C in Fig. 2(a)). Such type of anomalous responses was also observed above the Curie point in some tests (Fig. 4 is an example, which was a heating test at 10 Hz frequency in torsion vibration. The rate of temperature change was about 0.09 °C/s). These anomalies were neither attributed to the thermal gradient which was small (<3 °C), nor attributed to the experimental setup. Tests on a series of materials (including pure tin and alumina), which do not experience any transformation within the temperature and frequency regions concerned, with identical experimental configurations as for this $BaTiO_3$ ceramic specimen, have shown nothing anomalous.

3.3 DSC thermal analysis DSC results are shown in Fig. 5. Served as a comparison, the transition temperatures measured by means of BVS are provided inside the plot. The transition temperatures were taken by determining the starting temperatures of the peaks on the DSC curves and the mechanical loss curves. The transition temperature shifts as thermal rate is varied. The transition temperature in heating never converges to that in cooling however slow the thermal rate is achieved, even approaching zero. This phenomenon is called thermal hysteresis [11], a characteristic of first order phase transition. We infer the gap between the transition temperatures in a heating and a cooling process as the thermal rate is exponentially extrapolated to zero (a curve fitting in Fig. 5). This gap, which can be regarded as the thermal hysteresis region, was then found to be approximately 1.3 °C. The transition temperature is thus a small temperature region rather than one particular temperature point.

The transition temperature is lower in mechanical tests than that in thermal tests. Exponential extrapolation (curve

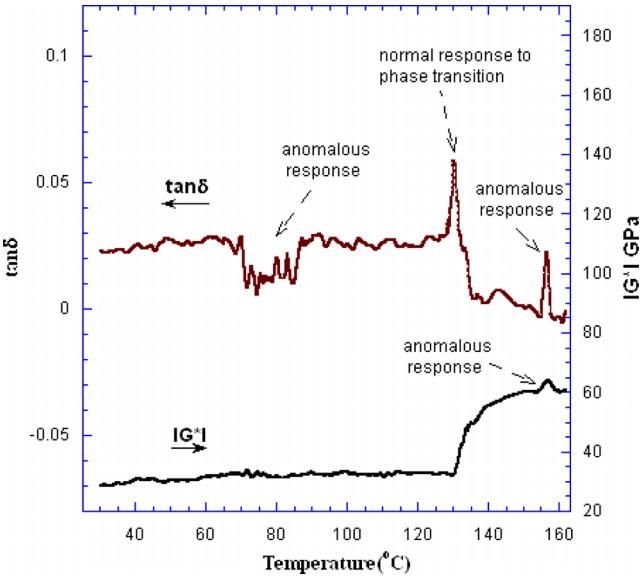

Figure 4 (online colour at: www.pss-b.com) An example exhibits the anomalous mechanical responses in polycrystalline $BaTiO_3$ above the Curie point. Test was performed at 10 Hz frequency in torsion vibration while the temperature was raised. The normal response at T_c to the phase transition was labeled to discriminate it from the anomalous responses.

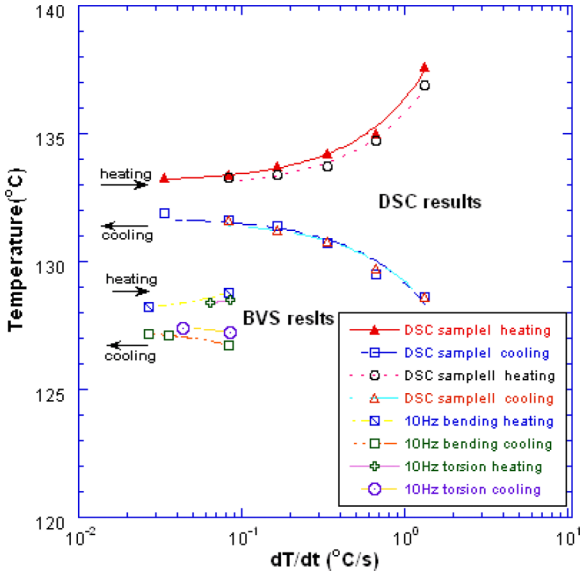

Figure 5 (online colour at: www.pss-b.com) Comparison of the transition temperatures, corresponding to the "tetragonal–cubic" phase transition in polycrystalline $BaTiO_3$, measured by DSC and via BVS. The transition temperatures were taken by determining the starting temperatures of the peaks on the DSC curves (DSC test) and the mechanical loss curves (BVS tests).

fitting in Fig. 5) was applied again to estimate the hysteresis region given thermo-mechanical coupling, which was found to be approximately 1.2 °C.

3.4 BVS isothermal frequency scans Isothermal frequency scans were conducted on this polycrystalline $BaTiO_3$ specimen from 10^{-3} Hz to approaching natural frequencies (590 Hz for bending and 5959 Hz for torsion), as shown in Figs. 6 and 7. For all the scans, the thermal gradient along the axial direction of the specimen and the thermal fluctuation of the hot air were less than 1.6 °C and 1 °C, respectively.

A hump on the mechanical loss curve below 1 Hz was observed within the transition temperature region. Away from the transition temperature, the loss tangent was more flat vs. frequency.

Young's modulus was found to have softened by a factor of ranging between 1.15 and 1.32 as frequency was reduced from 590 Hz to 10^{-3} Hz. A dip in Young's modulus was presented as $E_{124.6\,°C} > E_{126.5\,°C} < E_{128.5\,°C}$, and there was approximately 15 GPa reduction from $E_{124.6\,°C}$ (also $E_{128.5\,°C}$) to $E_{126.5\,°C}$. In the case of torsion, shear modulus was also observed to have softened by a factor of ranging from 1.13 to 1.23 as frequency was reduced from 3000 Hz to 10^{-3} Hz. The shear modulus, in contrast to Young's modulus, did not exhibit a relative minimum vs. temperature. Transformation process was found to be a function of time as a notable increment in moduli was often observed after a sufficiently long isothermal period in the vicinity of the phase transition. Observations have also shown that several hours of isothermal condition near the transition temperature enables the transformation to be completed. The measured moduli within this temperature region thus depended on the time under constant temperature.

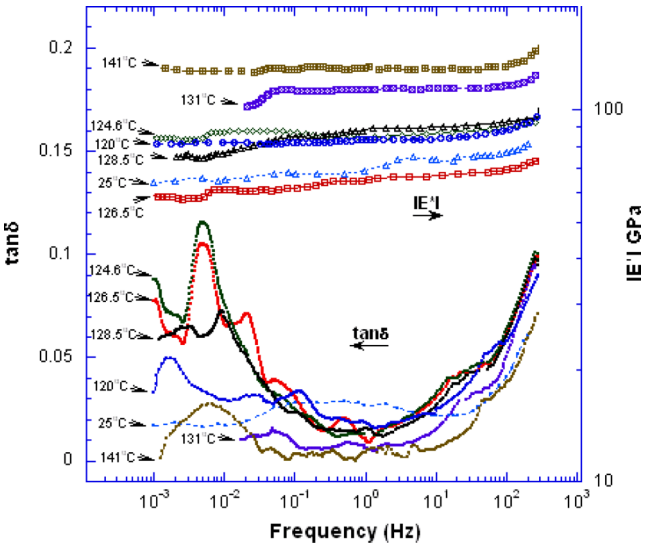

Figure 6 (online colour at: www.pss-b.com) Mechanical loss and Young's modulus vs. frequency curves of polycrystalline $BaTiO_3$ in isothermal frequency scans.

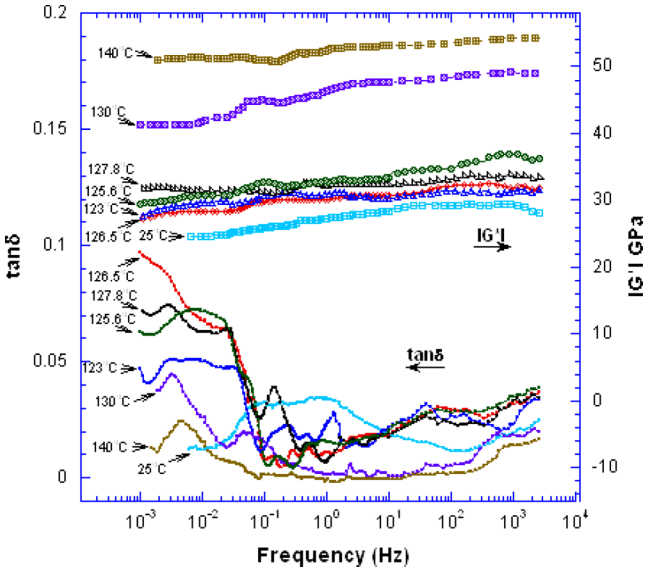

Figure 7 (online colour at: www.pss-b.com) Mechanical loss and shear modulus vs. frequency curves of polycrystalline $BaTiO_3$ in isothermal frequency scans.

3.5 BVS quasi-isothermal test Isothermal tests were conducted with the aims of isolating the effect of temperature from the effect of rate of temperature change, and of reducing temperature gradients along the specimen. Such tests take a long time (more than 1 hour). It is a painstaking task to maintain a constant temperature within narrow tolerance for such a long period. Moreover, varying frequency may disturb the process of the phase transition even under isothermal conditions, and thus blur the modulus defect. Furthermore, as shown in Fig. 5, the transition temperature in bending does not coincide exactly with that in torsion even at an identical thermal rate. Therefore, it is not that reasonable to calculate Poisson's ratio and bulk modulus based upon separate bending and torsion tests even though the thermal rate is well controlled to be identical. To avoid these problems, and to minimize the thermal gradient, shear modulus and Young's modulus were also measured quasi-isothermally (0.004 °C/s) at 10 Hz (far below natural frequencies) from 25 °C to 140 °C. At each temperature point, $|G^*|$ was measured prior to $|E^*|$ (Fig. 8). The thermal gradient along the specimen axial direction was less than 0.5 °C.

Polycrystalline $BaTiO_3$ is isotropic in nature due to the random orientation of the grains, therefore, the bulk modulus and Poisson's ratio can be calculated based upon the results (as shown in Fig. 8) by applying formulas (3) and (4) which are applicable to isotropic materials:

$$K = \frac{E}{9 - 3\dfrac{E}{G}}, \tag{3}$$

and

$$\nu = \frac{E}{2G} - 1, \tag{4}$$

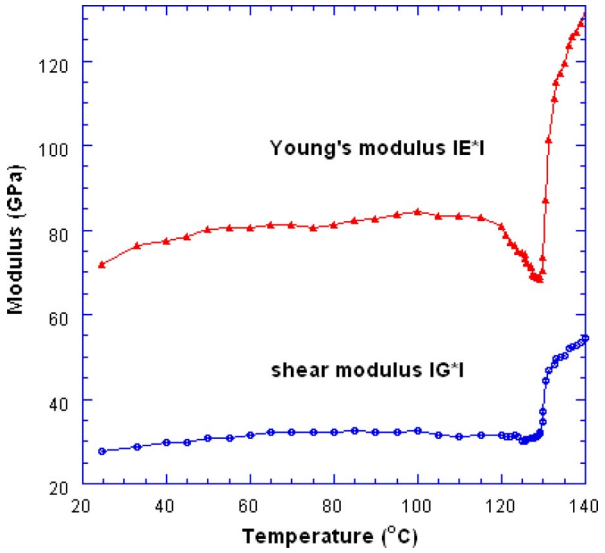

Figure 8 (online colour at: www.pss-b.com) Young's modulus and shear modulus vs. temperature of polycrystalline $BaTiO_3$ at 10 Hz frequency with a thermal rate of approximately 0.004 °C/s.

in which K, E, G, and v represent bulk modulus, Young's modulus, shear modulus, and Poisson's ratio, respectively (Fig. 9). Significant softening in bulk modulus (almost a factor of four) and reduction in Poisson's ratio (from 0.35 to a transient negative value −0.02) were disclosed during the phase transition. Slight softening in bulk modulus was also presented between 60 °C and 100 °C, corresponding to the anomalous mechanical responses as mentioned in the former part.

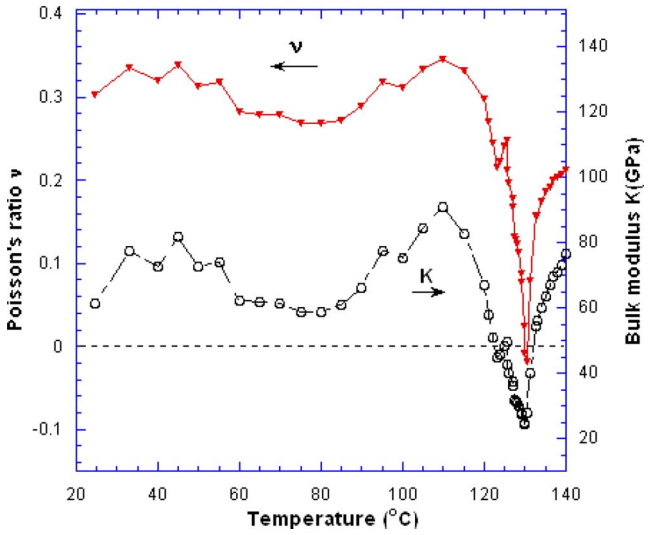

Figure 9 (online colour at: www.pss-b.com) Poisson's ratio and bulk modulus vs. temperature curves of polycrystalline $BaTiO_3$ at 10 Hz frequency, obtained from Fig. 8 by applying formulas (3) and (4).

4 Analysis and discussion

4.1 BVS temperature scans

4.1.1 Expressions for mechanical loss at the peak temperature Zhang et al. [10] explained FOPT from the perspective of the phase interface movement, and provided an expression for tan δ during the FOPT as:

$$\tan\delta = A(T)\,(T')^{g}/(2\pi f)^{g+2h} + B(T)\,(2\pi f)^{1-2h}\,, \tag{5}$$

in which $A(T)$ and $B(T)$ represent the mechanical loss of moving phase interface and the mechanical loss (independent of thermal rate) with static phase interface, i.e., the contribution from softening of phonon modes [10, 12], respectively. T' is of change in temperature; g and h are two parameters with $0 < g, h < 1$. g determines the dynamics of phase interface and the energy dissipation rate of FOPT [13], h is determined for the specific phase transition. f is frequency. Zhang et al. have applied this theory to explain many FOPT systems [10, 12], including $BaTiO_3$ ceramic [13] as it undergoes the two ferroelectric phase transitions below the Curie point. However, this model needs some revision since it only take into account the total free energy that drives the phase interface to move and the softening of phonon modes as the preconditions for the mechanical loss derivation during the FOPT, but has not considered the intrinsic damping of the system which does not originate from the mentioned free energy and the phonon modes softening. The intrinsic damping reflects how the nature of a specific phase of the real material deviates from ideal elasticity, and depends only on the microstructure of that specific phase [4].

Another well known model for tanδ during the martensitic transformation (a type of FOPT) is expressed as a sum of three contributions [4]:

$$\tan\delta = \tan\delta_{\text{transient}} + \tan\delta_{\text{PT}} + \tan\delta_{\text{intrinsic}}\,. \tag{6}$$

The magnitude of the transient term $\tan\delta_{\text{transient}}$ increases with increasing thermal rate and descending frequency. The second term $\tan\delta_{\text{PT}}$ comes from the phase transition itself, and still exists even when the thermal rate is reduced to zero. The third term $\tan\delta_{\text{intrinsic}}$ is the intrinsic damping of the parent and new phases that coexist during the phase transition. Although this model is proposed specifically for the martensitic transformation, it does reveal the nature of the mechanical loss during a FOPT in terms of all possible contributions.

By comparison of expressions (5) and (6) and the definition of each term, the following relations are suggested:

$$\tan\delta_{\text{transient}} = A(T)\,(T')^{g}/(2\pi f)^{g+2h}\,, \tag{7}$$

$$\tan\delta_{\text{PT}} = B(T)\,(2\pi f)^{1-2h}\,. \tag{8}$$

As a result, tan δ in (5) corresponds to ($\tan\delta_{\text{total}} - \tan\delta_{\text{intrinsic}}$). $\tan\delta_{\text{intrinsic}}$ of the system, which is found to be a weak function of thermal rate, is the weighted average of $\tan\delta_{\text{intrinsic}}$ of both the parent and the new phases. Figure 10 describes how to determine $\tan\delta_{\text{intrinsic}}$ of the system at temperature T

during the phase transition [4]. If one adds this intrinsic damping term into expression (5), we can obtain the expression for the total mechanical loss during the phase transition at the Curie point for this polycrystalline $BaTiO_3$ specimen:

$$\tan\delta = A(T)\,(T')^{g}/(2\pi f)^{g+2h} + B(T)\,(2\pi f)^{1-2h} + a(T)\cdot\tan\delta_{\text{intrinsicP}}(f, T_s) + (1 - a(T))\cdot\tan\delta_{\text{intrinsicN}}(f, T_f)\,, \quad (9)$$

in which $a(T)$ is the volume fraction of the parent phase remained in the system at temperature T during the phase transition, with $a(T_s) = 1$ and $a(T_f) = 0$. At T_p, the volume fraction of the parent phase remained in the system $a(T_p)$ is about 55% [12]. $\tan\delta_{\text{intrinsicP}}(f, T_s)$ and $\tan\delta_{\text{intrinsicN}}(f, T_f)$ are the intrinsic damping of the parent phase and the new phase at T_s and T_f of the transition, respectively, and are frequency dependent.

Peak values were used to derive the $\tan\delta_{T_p}$ expressions. First $\ln(\tan\delta/(\Delta M/M))$ was plotted against $\ln(2\pi f)$, and $-h$ was determined as the slope of the curve [13] (Fig. 11(a); $\Delta M/M$ refers to the modulus defect). Plot $\tan\delta/(2\pi f)^{1-2h}$ against $(T')^{g}/(2\pi f)^{1+g}$, subsequently, and g was defined as the value that gives the minimum root-mean-square error of the data points with respect to the least-squares fitting curve of this graph (i.e., linear curve fitting), the corresponding slope and intercept of this generated curve are $A(T_p)$ and $B(T_p)$, respectively [13] (Fig. 11(b)). Intrinsic dampings of the parent and new phases at T_s and T_f were found in approximation to exponentially increase with ascending frequency (10 Hz to 50 Hz) in the vicinity of the phase transition (Fig. 11(c) and (d)). Outside this frequency range, the relationship between the frequency and intrinsic damping may not be monotonic. Expressions for $\tan\delta$ can be readily obtained at this time as (1) and (2).

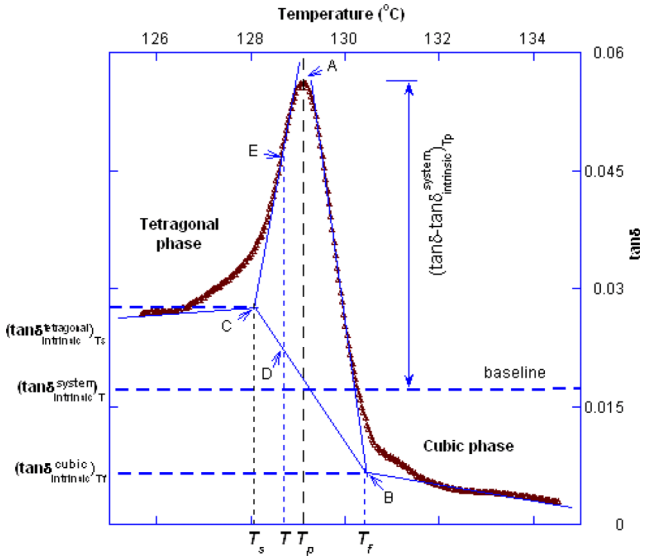

Figure 10 (online colour at: www.pss-b.com) A mechanical loss peak during the "tetragonal → cubic" phase transition in polycrystalline $BaTiO_3$. Measurement was performed at 10 Hz frequency in torsion vibration with approximately +0.07 °C/s thermal rate. Define $\tan\delta$ at T_s (starting temperature) and T_f (finishing temperature) of the phase transition as the intrinsic dampings of the parent and the new phases. At a specific temperature T during the transition, intrinsic damping $\tan\delta_{\text{intrinsic}}$ (i.e., baseline) is expressed as [4] $\tan\delta_{\text{intrinsic}} = a\cdot\tan\delta_{\text{intrinsicP}} + (1 - a)\cdot\tan\delta_{\text{intrinsicN}}$, in which a is the volume fraction of the parent phase remained in the system at temperature T. $\tan\delta_{\text{intrinsicP}}$ and $\tan\delta_{\text{intrinsicN}}$ are intrinsic dampings of the parent and the new phases at T, respectively. $(1 - a)$ can be obtained by referring to the ratio of the areas of two triangles as $A_{\Delta ECD}/A_{\Delta ACB}$ [12].

4.1.2 Anomalous responses in mechanical losses and moduli The mechanical anomalies (as indicated in Section 3.2) may be associated with the constrained negative stiffness of certain grains or domain aggregates. The effect of constraint on negative stiffness elements by adjacent structures is considered here in the light of the following observations on indium-thallium alloy (InTl) [14]. In polycrystalline InTl, negative-stiffness elements constraint effects were inferred based on the fact that the mechanical loss in the polycrystalline material exceeded that for single crystals of similar alloy. The high temperature portion of the mechanical loss peak in InTl occurs before any transgranular martensitic band was observed, therefore, this portion cannot be due to the interfacial motion. Constrained negative stiffness of the grains with local fine scale pre-martensitic bands can account for this mechanical loss. In polycrystalline $BaTiO_3$, a grain with multiple domains inside can be modeled as a system composed of a series of springs [15], and each domain serves as one spring. Negative stiffness is allowed for such a system if these springs are arranged in suitable configurations with sufficient constraint applied. Such an effect can also be realized in an aggregate of only a few domains. When torque is applied, each grain and domain inside the specimen cannot deform freely but in a way that conforms to the compatibility conditions for the grain and domain boundaries. Stored elastic energy is thus introduced. These anomalous responses may be attributed to the absorption or dissipation of the elastic energy between some constrained negative stiffness grains (with suitable multi-domain structure inside) or domain aggregates (with proper arrangements) and their surroundings under suitable conditions. The distribution of oxygen vacancies [6], preferably located at the grain and domain boundaries, may be one of the factors that determine these conditions, since it contributes to the compatibilities of the mechanical constraint boundaries. But could the anomalies observed above the Curie point be also associated with the constrained negative stiffness of grains or domain aggregates? Zhang et al. [16] have shown, by means of quantum mechanics, that the cubic phase in $BaTiO_3$ ceramic is also antiferroelectric, i.e., domain structure still exists above the Curie point. The present observation of the mechanical anomalies above the

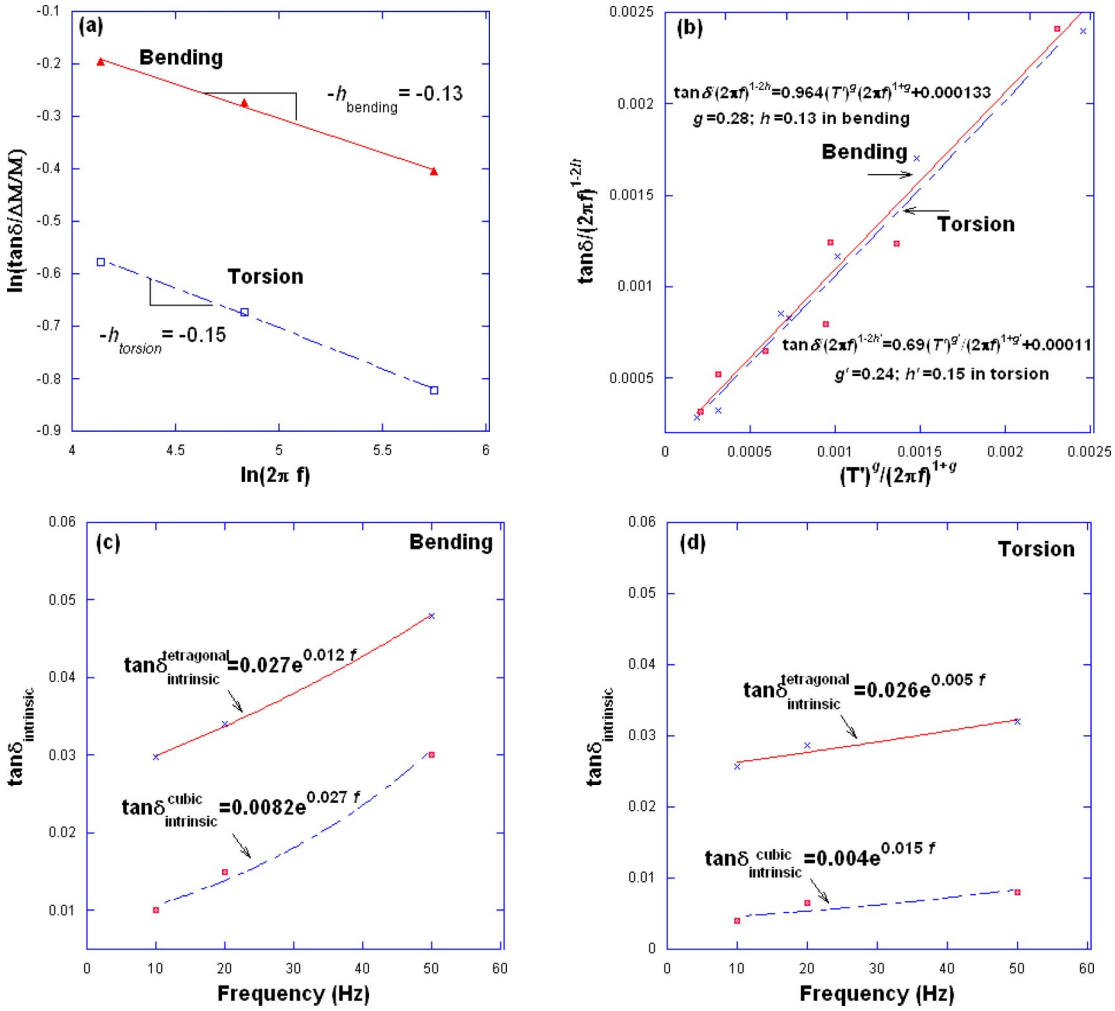

Figure 11 (online colour at: www.pss-b.com) (a) ln (tan $\delta/\Delta M/M$) vs. ln ($2\pi f$) curves during the "tetragonal → cubic" phase transition in polycrystalline $BaTiO_3$ in both bending and torsion vibrations. (b) tan $\delta/(2\pi f)^{1-2h}$ vs. $(T')^g/(2\pi f)^{1+g}$ curves during the "tetragonal → cubic" phase transition in both bending and torsion vibrations. (c) and (d) refer to the intrinsic dampings of the parent phase (tetragonal) and the new phase (cubic) at T_s and T_f of the "tetragonal → cubic" phase transition vs. frequency (from 10 Hz to 50 Hz) in both bending and torsion vibrations, respectively.

Curie point is in agreement with Zhang et al.'s conclusion, provided that such anomalies were indeed attributed to the effect of constrained negative stiffness.

Jaglinski et al. [3] have observed mechanical anomalies in the $BaTiO_3$–Sn composite materials within a narrow range of temperature far away from 130 °C, which corresponds to the "tetragonal ↔ cubic" phase transition of $BaTiO_3$, but much higher than its "orthorhombic ↔ tetragonal" phase transformation temperature around 10 °C. The size of the polycrystalline $BaTiO_3$ particle inclusions has a distribution between 15 μm and 210 μm (Fig. 2 of Ref. [3]), in which scale the Curie point is supposed to be around 130 °C [17]. If there were some inclusions (which would not be visible in the original micrograph) with grain size of less than 1 μm, the Curie point may be substantially reduced due to the enhanced surface energy. The observed temperature-shifted anomalies may be attributed to the "tetragonal ↔ cubic" phase transition of these tiny inclusions. Nevertheless, it is a possibility that the anomalies observed by Jaglinski et al. are linked to the anomalous behaviors as observed in this study of a polycrystalline $BaTiO_3$ specimen. Its bulk modulus at the temperature regions at which the mechanical anomalies were observed is unknown since $|E^*|$ and $|G^*|$ were measured in separate tests. If a sufficient softening in bulk modulus indeed occurred at these temperature regions, extreme mechanical properties are allowed by composite theory. Figure 9 does present a softening in bulk modulus between 60 °C and 100 °C though the measured $|E^*|$ and $|G^*|$ did not show apparent anomalies at that temperature region (Fig. 8).

4.2 Transition temperature (DSC vs. BVS) As for the divergence in the transition temperature between ther-

mal-induced and thermo-mechanical-induced transformations, it may be attributed to the internal stress. Ishidate et al. [18] have established a temperature-pressure phase diagram for polycrystalline $BaTiO_3$ by means of dielectric measurements. They have shown that the Curie point linearly decreases with increasing pressure up to 3 GPa, and the slope is approximately −55 °C/GPa. The rotation of grains and domains under dynamic loading introduces accumulating internal stress that preferably locates at the grain and domain boundaries. Such internal stress will exert pressure and thus lower the Curie point. As the level of the accumulated internal stress varies with different thermal and mechanical histories, the transition temperature in mechanical test could thus vary within a certain range. However, this stress-induced mechanism for the transition temperature shift is unlikely to account for the temperature regions (far away from 130 °C) at which the mechanical anomalies were observed in the $BaTiO_3$–Sn composite, as tin will yield at only 50 MPa, and that only correspond to less than one degree shift in the Curie point.

4.3 Moduli as a function of time in the vicinity of the phase transition in an isothermal condition As mentioned in Section 3.4, transformation can be gradually completed as time forwards at a constant temperature in the vicinity of the phase transition. First order phase transition is a process of nucleation and growth of the new phase from the parent phase [19], such a process is time dependent given an isothermal condition, i.e., the fraction of the new phase increases with time proportionally until the system is completely depleted of the parent phase. Besides, dynamic loading will accumulate internal stress. This internal stress reduces the transition temperature, and thus assists the progression of the transformation.

4.4 Modulus defect and lowering of Poisson's ratio during phase transformation in a quasi-isothermal condition As shown in Fig. 9, the bulk modulus exhibits a large softening of about a factor of four in the vicinity of the Curie point. However the softening does not proceed to zero. If the isotropic ceramic were to approach a negative bulk modulus (observable only under constraint) both the Young's modulus and the bulk modulus would soften to zero in an un-constrained sample, and the shear modulus would not soften significantly. Softening in the modulus will occur over a narrow range of temperature and composition, therefore good homogeneity of both temperature and composition is needed to observe the softening with fidelity. This is unlike the case of the composite for which only a dilute concentration of negative-stiffness inclusions is sufficient to obtain substantial effects [2]. Therefore, the extreme stiffness observed in the $BaTiO_3$-Sn composite does not necessarily require the participation of all the inclusions, and the thermal gradient in the composites is consequently a minor issue. Nonetheless, for this polycrystalline $BaTiO_3$ specimen, a significant softening in Young's modulus to zero was not observed. Lack of softening was not due to the thermal gradient for the following reasons. The thermal gradient in the cross-section of the specimen can be inferred by applying formula (10) [20]:

$$t = \frac{1}{4}\cdot\frac{d^2}{D} = \frac{1}{4}\cdot\frac{\rho C_p d^2}{k}, \tag{10}$$

in which t, d, D, k, C_p and ρ represent thermal diffusivity time constant, depth of penetration of heat in time t, thermal diffusivity, thermal conductivity, heat capacity and mass density, respectively. Given thermal conductivity of 4.7 W/(m K) [21], heat capacity of approximately 0.0006 J/(K kg) [9] when the "tetragonal ↔ cubic" transformation is undergoing, as well as mass density of 5.43×10^3 kg/m^3 for this specimen, thermal diffusion was found to be about 1.5 mm^2 s^{-1}. For a cross section of 2.447 × 2.78 mm, heat transfer could thus be completed within 0.4 s. As when the thermal rate is reduced to 0.004 °C/s, thermal gradient in the cross section can be neglected. Further effort led to the reduction of thermal gradient to within 0.1 °C (with thermal rate of approximately 0.003 °C/s), but further softening in Young's modulus was not observed (Fig. 12).

Polycrystalline bulk material inevitably has local structural and compositional inhomogeneities. Furthermore, bulk material contains pores and microcracks, which operate as stress concentrators. These factors lead to the non-uniformity in the transition temperature for different parts of the specimen. Additionally, internal strain would induce variation in the transition temperature by referring to the Landau's theory of phase transition [22]. Total free energy is then the sum of the bulk Landau free energy and the elastic energy [23]. Elastic energy induced by a torsion

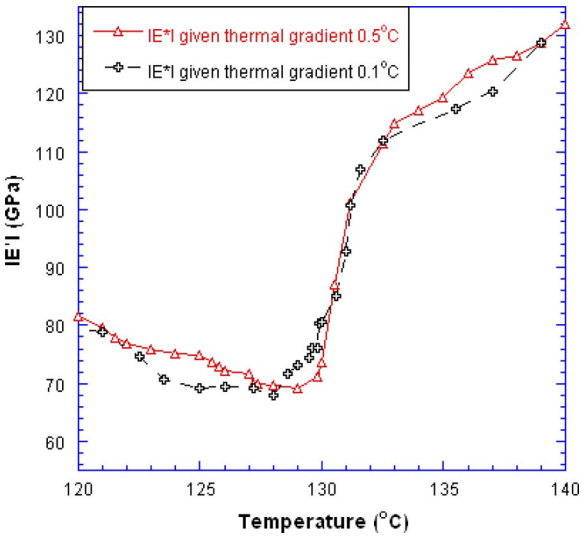

Figure 12 (online colour at: www.pss-b.com) Comparison of Young's modulus of polycrystalline $BaTiO_3$ in the vicinity of the phase transition near the Curie point as the thermal gradient was reduced from 0.5 °C to 0.1 °C. Similar thermal rates (0.003–0.004 °C/s) were applied for both measurements.

torque is different from that by a bending torque. However, such a difference in elastic energy could disturb the process of the phase transition even isothermally, thus influence the measured $|E^*|$ and $|G^*|$. Slow thermal rate could be another reason. Modulus defect during the FOPT originates from the moving interface and the softening of phonon modes [10]. Though the contribution to modulus defect from the phonon modes softening is independent of the thermal rate [24], phase interface velocity will decrease as the thermal rate is reduced [10]. As a result, the modulus defect may not be as prominent as when a high thermal rate is applied.

Softening in elastic constants was reported in several types of single crystal ceramics [25–27] when they undergo phase transitions while electrically short-circuited. As for the $BaTiO_3$–Sn composite material, a portion of particles are able to exist in the form of single crystals. Also, these particles are surrounded by metallic matrix, and the electric boundary condition of uniform potential is thus available. For $BaTiO_3$ single crystal, bulk moduli in the tetragonal phase (possesses transversely isotropic symmetry) and the cubic phase (possesses isotropic symmetry) are expressed in terms of elastic constants as formulas (11) and (12) [28]:

$$K_{\text{Tetragonal}} = \left(\frac{C_{33}(C_{11}+C_{12}) - 2C_{13}^2}{2C_{33} + C_{11} + C_{12} - 4C_{13}} \right)_{\text{Tetragonal}} \tag{11}$$

and

$$K_{\text{Cubic}} = \left(\frac{C_{11} + 2C_{12}}{3} \right)_{\text{Cubic}} \tag{12}$$

and when the phase transition takes place, convergence of elastic constants is expressed as $[(C_{33})_{\text{Tetragonal}} \neq (C_{11})_{\text{Tetragonal}}] \rightarrow (C_{11})_{\text{Cubic}}$ and $[(C_{13})_{\text{Tetragonal}} \neq (C_{12})_{\text{Tetragonal}}] \rightarrow (C_{12})_{\text{Cubic}}$. In contrast, polycrystalline $BaTiO_3$ possesses isotropic symmetry in a statistical sense although anisotropic microscopically. As a result, bulk moduli are expressed as (13) and (14):

$$K_{\text{Tetragonal}} = \left(\frac{\langle C_{11} \rangle + 2\langle C_{12} \rangle}{3} \right)_{\text{Tetragonal}} \tag{13}$$

and

$$K_{\text{Cubic}} = \left(\frac{\langle C_{11} \rangle + 2\langle C_{12} \rangle}{3} \right)_{\text{Cubic}} . \tag{14}$$

In Eq. (13), $\langle C_{11} \rangle_{\text{Tetragonal}}$, $\langle C_{12} \rangle_{\text{Tetragonal}}$ are functions of $(C_{ij})_{\text{Tetragonal}}$ of the single crystal, the expressions of which are very complex, and there is no unique relationship between the bulk modulus of single crystal and that of polycrystalline [29]. However, in Eq. (14), the isotropy condition $\langle C_{44} \rangle_{\text{Cubic}} = 1/2(\langle C_{11} \rangle_{\text{Cubic}} - \langle C_{12} \rangle_{\text{Cubic}})$ is satisfied after averaging, and the single crystal and polycrystalline bulk moduli are equal [30]. Furthermore, if the effects from the structural and compositional inhomogeneities as well as the existence of defects are taken into account, the expressions for the bulk moduli of the polycrystalline $BaTiO_3$ would be more complicated.

With sufficient constraint from the surrounding matrix [3], negative bulk modulus of the inclusions can be restrained for a certain time interval and thus be revealed, which is the not the case as for this polycrystalline $BaTiO_3$ specimen as when it undergoes the corresponding phase transition. Nevertheless, if sufficient constraint is available, negative Young's modulus may be able to be stabilized.

Figure 9 also presents a transient lowering in Poisson's ratio to a slightly negative value in the vicinity of the phase transformation. Negative Poisson's ratio behavior has been earlier observed experimentally in polymer gels [31, 32] near the volume phase transition, and studied by computer simulations [33] in several single-disperse and polydisperse hard disc systems. Negative Poisson's ratio also occurs in designed foams, via unfolding of the cells [34]. Poisson's ratio is an indicator of mechanical stability of isotropic solids [33], and it is very interesting to observe a negative Poisson's ratio in a stiff polycrystalline material in the vicinity of phase transformation. When the Poisson's ratio becomes negative and approaches –1, the bulk modulus will become less than the shear modulus and gradually approaches zero [15, 35]. Simulations [33] have predicted that a more homogeneous grain size distribution and a lower degree of defect concentration will help to lower the Poisson's ratio of the system in the vicinity of mechanical instability.

5 Conclusion Polycrystalline $BaTiO_3$ was studied in torsion and bending over a range of temperature and frequency. A peak in mechanical loss has been observed at the Curie point. The height and width of the peak increase with thermal rate and the inverse of frequency, in harmony with theory. Anomalous responses in mechanical losses and moduli were observed in some temperature scans outside the transition temperature regions. Damping maxima were observed at low frequency in isothermal studies near the Curie point. Thermal hysteresis during the transformation, whether measured via scanning calorimetry or via mechanical spectroscopy, was found to be approximately 1.3 °C. Bulk modulus softened by about a factor of four near the Curie point, and Poisson's ratio attained a slightly negative value. The softening may have been broadened by compositional and structural heterogeneities.

References

[1] Z. Hashin and S. Shtrikman, J. Mech. Phys. Solids **11**, 127–140 (1963).
[2] R. S. Lakes, Phys. Rev. Lett. **86**, 2897–2900 (2001).
[3] T. Jaglinski, D. Kochmann, D. S. Stone, and R. S. Lakes, Science **315**, 620–622 (2007).
[4] R. B. Pérez-Sáez, V. Recarte, M. L. Nó, and J. San Juan, Phys. Rev. B **57**, 5684–5692 (1997).
[5] B. L. Cheng, M. Gabbay, M. Maglione, and G. Fantozzi, J. Electroceram. **10**, 5–18 (2003).

[6] B. L. Cheng, M. Gabbay, W. Duffy, and G. Fantozzi, J. Mater. Sci. **31**, 4951–4955 (1996).
[7] T. Lee, R. S. Lakes, and A. Lal, Rev. Sci. Instrum. **71**, 2855–2861 (2000).
[8] F. Kulcsar, J. Am. Ceram. Soc. **39**, 13–17 (1956).
[9] F. Jona and G. Shirane, Ferroelectric Crystals, International Series of Monographs on Solid State Physics (Pergamon Press, Oxford, 1962), chap. 4, pp. 123–125.
[10] J. X. Zhang, P. C. W. Fung, and W. G. Zeng, Phys. Rev. B **52**, 268–277 (1995).
[11] W. L. Zhong, First-order ferroelectric phase transformation, in: Ferroelectric Physics (Science Press, China, 1996).
[12] J. X. Zhang, Z. H. Yang, and P. C. W. Fung, Phys. Rev. B **52**, 278–284 (1995).
[13] J. X. Zhang, W. Zheng, P. C. W. Fung, and K. F. Liang, J. Alloys Compd. **211/212**, 378–380 (1994).
[14] T. Jaglinski, P. Frascone, B. Moore, D. S. Stone, and R. S. Lakes, Philos. Mag. **86**, 4285–4303 (2006).
[15] Y. C. Wang and R. S. Lakes, J. Compos. Mater. **39**, 1645–1657 (2005).
[16] Q. S. Zhang, T. Cagin, and W. A. Goddard, Proc. Natl. Acad. Sci. USA **103**, 14695–14700 (2006).
[17] M. H. Frey and D. A. Payne, Phys. Rev. B **54**, 3158–3169 (1996).
[18] T. Ishidate, S. Abe, H. Takahashi, and N. Mori, Phys. Rev. Lett. **78**, 2397–2400 (1997).
[19] Y. Yamada, N. Hamaya, J. D. Axe, and S. M. Shapiro, Phys. Rev. Lett. **53**, 1665–1668 (1984).
[20] J. F. Ready, Interaction of high-power laser radiation with material, in: Industrial Application of lasers, 2nd edition (Academic Press, New York, 1997), chap. 12, p. 316.
[21] A. J. H. Mante and J. Volger, Phys. Lett. A **24**, 139–140 (1967).
[22] L. D. Landau, in: Collected Papers of L. D. Laudau, edited by D. Ter Taar (Gordon and Breach/Pergamon Press, New York, 1965), pp. 193–216.
[23] Y. L. Li, S. Choudhury, J. H. Haeni, M. D. Biegalski, A. Vasudevarao, A. Sharan. H. Z. Ma, J. Levy, V. Gopalan, S. T. Mckinstry, D. G. Schlom, Q. X. Jia, and L. O. Chen, Phys. Rev. B **73**, 184112–184125 (2006).
[24] R. Blinc and B. Zeks, Soft modes in ferroelectrics and antiferroelectrics (North-Holland Pub. Co., Amsterdam, Oxford, 1974).
[25] E. Litov and E. A. Uehling, Phys. Rev. Lett. **21**, 809–812 (1968).
[26] E. M. Brody and H. Z. Cummins, Phys. Rev. Lett. **21**, 1263–1266 (1968).
[27] B. Kinder, D. Finsterbusch, R. Graf, F. Ritter, W. Assmus, and B. Luthi, Phys. Rev. B **50**, 704–708 (1994).
[28] A. Ballato, IEEE Trans. Ultrason. Ferroelectr. Freq. Control **43**, 56–62 (1996).
[29] H. M. Ledbetter and E. R. Naimon, J. Appl. Phys. **45**, 66–69 (1974).
[30] K. S. Mendelson, J. Phys. D **14**, 1307–1309 (1981).
[31] S. Hirotsu, J. Chem. Phys. **94**, 3949–3957 (1991).
[32] S. Hirotsu, Macromolecules **23**, 903–905 (1990).
[33] K. V. Tretiakov and K. W. Wojciechowski, phys. stat. sol. (b) **242**, 730–741 (2005).
[34] R. S. Lakes, Science **235**, 1038–1040 (1987).
[35] I. S. Sokolnikoff, Mathematical Theory of Elasticity (Krieger Publ. Co., Malabar, Florida, 1983).

